THE JOURNAL OF BIOLOGICAL CHEMISTRY VOL. 290, NO. 27, pp. 16665–16677, July 3, 2015

Members of the Plant CRK Superfamily Are Capable of Trans- and Autophosphorylation of Tyrosine Residues*[S]

Received for publication, October 9, 2014, and in revised form, May 11, 2015 Published, JBC Papers in Press, May 12, 2015, DOI 10.1074/jbc.M114.617274

Keiichirou Nemoto[‡], Nobuaki Takemori[‡], Motoaki Seki[§‖], Kazuo Shinozaki[¶], and Tatsuya Sawasaki[‡1]

From the [‡]Proteo-Science Center, Ehime University, 3 Bunkyo-cho, Matsuyama, Ehime 790-8577 and the [§]Plant Genomic Network Research Team and the [¶]Gene Discovery Research Group, RIKEN Center for Sustainable Resource Science, 1-7-22 Suehiro-cho, Tsurumi-ku, Yokohama, Kanagawa 230-0045, and [‖]CREST, Japan Science and Technology Agency (JST), 4-1-8 Honcho, Kawaguchi, Saitama 332-0012, Japan

Background: Protein kinases that catalyze Tyr phosphorylation in plants *in vivo* are largely unknown.
Results: CDPK/CPK-related protein kinases (CRKs) that auto/trans-phosphorylate Tyr residues and six substrates of these were identified. CRK knock-out mutants show reduced Tyr phosphorylation of β-tubulin proteins.
Conclusion: CRKs can phosphorylate Tyr residues of β-tubulin and certain transcription factors.
Significance: CRKs might be responsible for much of the protein Tyr phosphorylation *in vivo*.

Protein phosphorylation on Tyr residues is a key post-translational modification in mammals. In plants, recent studies have identified Tyr-specific protein phosphatase and Tyr-phosphorylated proteins in *Arabidopsis* by phosphoproteomic screenings, implying that plants have a Tyr phosphorylation signal pathway. However, little is known about the protein kinases (PKs) involved in Tyr phosphorylation in plants. Here, we demonstrate that *Arabidopsis* calcium-dependent protein kinase (CDPK/CPK)-related PKs (CRKs) have high Tyr-autophosphorylation activity and that they can phosphorylate Tyr residue(s) on substrate proteins in *Arabidopsis*. To identify PKs for Tyr phosphorylation, we examined the autophosphorylation activity of 759 PKs using an *Arabidopsis* protein array based on a wheat cell-free system. In total, we identified 38 PKs with Tyr-autophosphorylation activity. The CRK family was a major protein family identified. A cell-free substrate screening revealed that these CRKs phosphorylate β-tubulin (TBB) 2, TBB7, and certain transcription factors (TFs) such as ethylene response factor 13 (ERF13). All five CRKs tested showed Tyr-auto/trans-phosphorylation activity and especially two CRKs, CRK2 and CRK3, showed a high ERF13 Tyr-phosphorylation activity. A cell-based transient expression assay revealed that Tyr^{16}/Tyr^{207} sites in ERF13 were phosphorylated by CRK3 and that Tyr phosphorylation of endogenous TBBs occurs in CRK2 overexpressing cells. Furthermore, *crk2* and *crk3* mutants showed a decrease in the Tyr phosphorylation level of TBBs. These results suggest that CRKs have Tyr kinase activity, and these might be one of the major PKs responsible for protein Tyr phosphorylation in *Arabidopsis* plants.

Protein phosphorylation of serine (Ser), threonine (Thr), and tyrosine (Tyr) residues is a key post-translational modification required for signal transduction in eukaryotes. In animals, protein-tyrosine kinases (PTKs)[2] play a central role in many signaling pathways, including hormone response, differentiation, development, and cancer formation (1). In contrast, it is unclear whether Tyr phosphorylation signaling cascades exist in plants, because no PTK homologous genes have been reported in *Arabidopsis* and rice genomes (2, 3).

Recently, Tyr-specific protein phosphatase (PTP1) (4) and more than 1000 Tyr-phosphorylated proteins have been identified by proteomics analysis (5, 6) in plants. A previous report suggests that not only PTP1 but also dual-specific (pSer/pThr and pTyr) phosphatases involve in abiotic stress and hormone signaling are present in plants (7). On the other hand, a phosphoproteomic approach revealed that ~4% of phosphopeptides are Tyr-phosphorylated peptides in plants and the proportion of Tyr phosphorylation is equivalent to that found in human cells (5). In addition, *meta*-analysis of phosphoproteomic data revealed that Tyr-phosphorylated peptides are overrepresented in mitochondrial and characterized two Tyr phosphorylation motifs (6). Other studies have demonstrated that PTK and PTP inhibitor application to plants alter abscisic acid (8), gibberellin (9), cold stress (10), and sugar responses (11), as well as cytoskeleton organization (12) and cell division (13). These findings strongly suggest that plants possess Tyr phosphorylation signaling pathways. According to recent studies, Tyr residues (as well Ser and Thr) of several dual-specific (Ser/Thr/Tyr) type or Ser/Thr-specific type PKs, *e.g.* receptor-like/receptor-like cytoplasmic PKs (RLK/RLCKs), CDPKs, glycogen synthase kinase 3 (GSK3)/Shaggy-like PKs, and MAPK have been observed to autophosphorylate (14–16). These PKs probably participate in Tyr phosphorylation signaling in plants.

* This work was supported by a Grant-in-Aid for Scientific Research (B) (to T. S.) and the Platform for Drug Discovery, Informatics, and Structural Life Science (to T. S.) and a Grant-in-Aid for Scientific Research on Innovative Areas (to T. S.) from the Ministry of Education, Culture, Sports, Science, and Technology in Japan. The authors declare that they have no conflicts of interest with the contents of this article.

The mass spectrometry proteomics data have been deposited to the ProteomeXchange Consortium via the PRIDE partner repository (68) with the data set identifier PXD002158.

[S] This article contains supplemental Tables S1–S4.

[1] To whom correspondence should be addressed. Tel.: 81-89-927-8530; Fax: 81-89-927-9941; E-mail: sawasaki@ehime-u.ac.jp.

[2] The abbreviations used are: PTK, protein-tyrosine kinase; PK, protein kinase; CDPK/CPK, calcium-dependent protein kinase; CRK, CDPK/CPK-related protein kinase; TBB, β-tubulin; ERF13, ethylene response factor 13; PTP1, tyrosine-specific protein phosphatase 1; TF, transcription factor; PPI, protein-protein interaction; KD, kinase dead; MT, microtubule; GSK, glycogen-synthase kinase 3; RLK/RLCK, receptor-like/receptor-like cytoplasmic PK.

However, the molecular mechanisms of signaling pathways that are controlled by Tyr phosphorylation remain to be clarified because the substrate proteins for Tyr phosphorylation have not been identified.

To understand the Tyr phosphorylation signaling, it is important to identify PKs and their substrate protein for Tyr phosphorylation. Although PKs are one of the largest gene families, representing ~4% (more than 1,000) of all the genes in *Arabidopsis* and rice, the biochemical characteristics of most plant PKs are unclear. In our previous study (17), we demonstrated the Ser/Thr autophosphorylation activity using a high-throughput profiling method combining the *Arabidopsis* 759 PKs array that was produced using a wheat cell-free system, and a luminescent method "AlphaScreen." Here, by modifying this approach, we have identified and characterized 38 Tyr autophosphorylation PKs. Among them, we focused on angiosperm-specific CRK2, CRK3, and CRK8, and screened for the substrate protein for Tyr phosphorylation using a TFs protein array (18) and a pulldown assay using cellular extracts. We identified 6 substrate proteins in total. Cell-based transient expression assay and analysis of *crk2* and *crk3* mutants revealed that CRK2 and CRK3 were able to phosphorylate Tyr residue(s) of substrate proteins such as TBBs or ERF13 in cells or plants. In addition, the five proteins tested from the CRK family showed Tyr-auto/trans-phosphorylation activity *in vitro*. These findings suggest that CRK proteins possibly function as PKs for Tyr phosphorylation in plants.

Experimental Procedures

General—The following procedures were previously described (19–22): wheat cell-free protein production, split-primer PCR for construction of the DNA templates, parallel syntheses of mRNAs and their translated proteins, protein biotinylation, purification of synthesized proteins, hydrolysis of radioisotope-labeled protein, and quantification of proteins synthesized using densitometer scans of Coomassie Brilliant Blue-stained proteins or radiolabeled proteins.

Analysis of Protein Kinase Autophosphorylation Using a Luminescent Method—In vitro autophosphorylation assays were carried out as previously described with slight modifications (17). Ser/Thr or Tyr autophosphorylation was detected by anti-phospho-Ser/Thr (Upstate Biotechnology, Lake Placid, NY) or anti-phospho-Tyr antibody (4G10) (Millipore), respectively. All data represent the average of two independent experiments and the background for each experiment was controlled using the relevant non-biotinylated PK. For *in vitro* dephosphorylation assays, autophosphorylated biotinylated PKs were incubated with crude FLAG-PTP1 at 26 °C for 60 min. Tyr autophosphorylation was detected by anti-phospho-Tyr antibody (4G10). All data represent the average of three independent experiments, and dephosphorylation efficiency was defined as the ratio of PTP1-treated kinases to untreated kinases.

Phosphoamino Acid Analysis—The phosphoamino acid analysis was performed according to a previous method (23). Biotinylated PKs were purified using streptavidin MagneSphere® Paramagnetic Particles (Promega), and incubated at 30 °C for 30 min in a total volume of 50 μl consisting of 50 mM Tris-HCl (pH 7.6), 37 kBq of [γ-^{32}P]ATP, 100 mM potassium acetate, 10 mM $MgCl_2$, and 1 mM DTT. Then, biotinylated PKs were hydrolyzed using 6 N HCl at 110 °C for 4 h. After drying the product, each amino acid was separated by thin-layer chromatography (TLC) using ethanol:ammonium hydroxide:water at a ratio of 105:42:6 (v/v) and each ^{32}P-labeled amino acid was detected by autoradiography.

In Vitro Phosphorylation and Dephosphorylation Assays—For *in vitro* kinase assays, biotinylated proteins and FLAG-tagged proteins were purified using streptavidin MagneSphere® Paramagnetic Particles and anti-FLAG M2-agarose (Sigma), respectively. Then, *in vitro* kinase assays were carried out in a total volume of 50 μl consisting of 50 mM Tris-HCl (pH 7.6), 100 mM potassium acetate, 10 mM $MgCl_2$, 1 mM DTT, and 100 μM ATP or 37 kBq of [γ-^{32}P]ATP at 26 °C for 30–60 min. Dephosphorylation by AtPTP1 was carried out in a total volume of 50 μl consisting of 50 mM Tris-HCl (pH 7.5), 10 mM $MgCl_2$, 2 mM DTT, 0.01% Brij 35, and 50 ng of purified FLAG-AtPTP1 at 26 °C for 30–60 min. For immunoblotting, anti-phospho-Tyr antibody (4G10) was used to detect phosphotyrosine. Biotinylated proteins were detected with Alexa Fluor 647 streptavidin conjugate (Invitrogen). The chemiluminescent signal, fluorescent signals, and filmless autoradiography were detected using an ImageQuant LAS-4000 mini biomolecular imager (GE Healthcare), a Typhoon 9400 imager (GE Healthcare) with a 633-nm laser and a 670-nm BP30 emission filter, and a Typhoon FLA 9000 phosphorimager (GE Healthcare), respectively.

In-Gel Protein Digestion—Coomassie Brilliant Blue-stained protein bands were excised from the SDS-PAGE gels and further destained using 50% (v/v) acetonitrile in 100 mM ammonium bicarbonate (pH 8.9). Destained gel pieces in 30 μl of 100 mM ammonium bicarbonate (pH 8.9) were reduced by adding 10 μl of 40 mM dithiothreitol for 2 h at 37 °C and alkylated by adding 10 μl of 250 mM acrylamide for 30 min at room temperature. In-gel digestion of each protein was performed with 0.1 μg of sequencing grade modified trypsin or chymotrypsin (Promega, Madison, WI) at 37 °C for 12 h. After repeated extractions of tryptic digests from the gel with 50% (v/v) acetonitrile, 5% (v/v) trifluoroacetic acid, the solution containing the extracted peptides was concentrated using a vacuum microcentrifuge. The peptide sample was reconstituted with 0.1% (v/v) trifluoroacetic acid for mass spectrometry (MS) analysis.

Liquid Chromatography-Mass Spectrometry Analysis—Tandem MS (MS/MS) analysis was performed using the LTQ XL linear ion trap mass spectrometer (Thermo Fisher Scientific) coupled with DiNa nano LC system (KYA Technologies). Peptide separations were performed at a constant flow rate of 300 nl/min with a fused silica capillary column packed with C18 resin (75 μm × 15 cm). Mobile phases used for separation were 0.1% formic acid (A) and 80% acetonitrile with 0.1% formic acid (B). A gradient (2–50% mobile phase B) was applied for 25 min, followed by a 10-min wash at 100% mobile phase B, and a equilibration for 15 min with 2% mobile phase B. For the identification of autophosphorylation sites, MS/MS spectra were processed using the Proteome Discoverer software version 1.1 (Thermo Fisher Scientific). Peptide identification was performed using the SEQUEST search algorithm with the follow-

ing parameters: two missed cleavages were allowed; precursor mass tolerance, 2 Da; fragment mass tolerance, 0.8 Da; static modification, propionamide (cysteine); dynamic modifications, phosphorylation (serine, threonine, and tyrosine), methionine oxidation, and pyroglutamic acid. For the identification of substrate proteins, the acquired MS/MS spectra were searched against the IPI *Arabidopsis* database (ipi.ARATH version 3.85) using the SEQUEST software and we required at least one high-quality peptide for positive identification (peptide probability score ≥10).

Construction of Transient Expression Plasmids for Cultured Cells—Full-length cDNAs of *CRK2*, *CRK3*, and *ERF13* were cloned into pDONR221 vectors via Gateway reactions. After the clone sequence was confirmed, the C-terminal HA-tagged form and kinase dead (K_D) form mutants, CRK2 (Lys^{176} to Arg) and CRK3 (Lys^{175} to Arg), were generated using a PrimeSTAR Mutagenesis Basal kit (Takara Bio) according to the manufacturer's instructions. Fragments containing the gene coding sequence and the HA tag were subcloned into p35SΩ-GW-NOST vectors (which we generated from the 35SΩ-sGFP vector (24)),[3] using LR clonase reaction (Invitrogen). We produced expression vectors for YFP or GFP fusion proteins by LR clonase recombination of CRK2 or CRK3 and p35SΩ-GW-YFP-NOST vectors, and ERF13 and p35SΩ-GW-GFP-NOST vectors.

Tyr Phosphorylation Analysis of Substrate Proteins and Subcellular Localization Analysis by Transient Expression—Isolation of *Arabidopsis* suspension-cultured cell protoplasts and polyethylene glycol-mediated DNA transfection were performed as previously described (25). For Tyr phosphorylation analysis of ERF13-GFP, 100 μg of plasmid DNA of ERF13-GFP and 40 μg of plasmid DNA of CRK2-HA or CRK3-HA were transfected into 2×10^6 protoplasts. After overnight incubation in the dark, crude extracts were obtained by homogenizing protoplasts in radioimmunoprecipitation assay buffer supplemented with phosphatase inhibitor mixture (PhosSTOP, Roche) and protease inhibitor mixture (Sigma). Immunoprecipitation of ERF13-GFP was performed with 50 μl of Protein G-Sepharose (GE Healthcare) and 1 μl of rabbit polyclonal anti-GFP antibody (MBL), and aliquots were analyzed by immunoblot analysis using rabbit polyclonal anti-GFP antibody or anti-phospho-Tyr antibody (4G10). For Tyr phosphorylation analysis of endogenous TBBs, 40 μg of plasmid DNA of CRK2-HA or CRK3-HA was used for transfection, and crude extracts were obtained in cell lysis buffer (20 mM Tris-HCl (pH 7.5), 150 mM NaCl, 1 mM EDTA, 1 mM EGTA, 1% Triton X-100, phosphatase inhibitor mixture, and protease inhibitor mixture). Immunoprecipitation of endogenous TBBs was performed with 50 μl of Protein G-Sepharose and 5 μl of mouse polyclonal anti-TBB antibody (TUB2.1) (Sigma), and aliquots were analyzed by Phos-Tag SDS-PAGE (100 μM Phos-Tag and 100 μM $MnCl_2$) and immunoblot analysis using mouse polyclonal anti-TBB antibody or anti-phospho-Tyr antibody (4G10). Expression of CRK2-HA and CRK3-HA was detected by anti-HA-HRP antibody (3F10) (Roche Applied Science). For subcellular localization analysis, 10 μg of plasmid DNA was transfected to 100 μl of 2×10^4 protoplasts. YFP and GFP fluorescence was observed with a confocal laser-scanning microscope LSM5 PASCAL (Zeiss).

Identification of Tyr-phosphorylated Proteins from Extracts of Arabidopsis Cultured Cells—For substrate screening by co-immunoprecipitation, biotinylated CRK3 was attached to streptavidin MagneSphere® Paramagnetic Particles (Promega). After washing, CRK3 was incubated with *Arabidopsis* suspension-cultured cells lysate in immunoprecipitation buffer (25 mM Tris-HCl, 150 mM NaCl, 0.5% Triton X-100, phosphatase inhibitor mixture, and protease inhibitor mixture) at 26 °C for 60 min. Following the above reaction, the beads were washed 4 times with immunoprecipitation buffer, and then boiled in the sample buffer. The precipitated interacting proteins were analyzed by immunoblotting with anti-phospho-Tyr antibody, Coomassie Brilliant Blue stain, and MS analysis.

Identification of Tyr-phosphorylated Proteins Using Protein Library of Arabidopsis TFs—For substrate screening using AlphaScreen, 188 TFs were selected from the *Arabidopsis* TF library previously described (18). *In vitro* protein-protein interaction (PPI) assays were carried out in a total volume of 15 μl consisting of 100 mM Tris-HCl (pH 8.0), 0.1% Tween 20, 1 mg/ml of BSA, 1 μl of biotinylated TFs, and FLAG-PKs at 25 °C for 1 h in a 384-well Optiplate (PerkinElmer Life Sciences). In accordance with the AlphaScreen IgG (Protein A) detection kit (PerkinElmer) instruction manual, 10 μl of detection mixture containing 100 mM Tris-HCl (pH 8.0), 0.1% Tween 20, 1 mg/ml of BSA, 5 μg/ml of anti-FLAG M2 antibody (Sigma), 0.1 μl of streptavidin-coated donor beads, and 0.1 μl of Protein A-coated acceptor beads was added to each well of the 384-well Optiplate, followed by incubation at 25 °C for 1 h. Luminescence was analyzed using the AlphaScreen detection program. All data represent the average of two independent experiments and the background was controlled using a dihydrofolate reductase from *Escherichia coli*.

Mutational Analysis—Mutagenesis was carried out using a PrimeSTAR Mutagenesis Basal kit (Takara Bio) according to the manufacturer's instructions. The mutated genes were sequenced using an ABI PRISM 310 DNA sequencer (Applied Biosystems).

T-DNA-tagged Line Analysis—T-DNA insertion mutant lines for *crk2* and *crk3* were obtained from the *Arabidopsis* Biological Resource Center. The *crk2* (Salk_090938C) and *crk3* (Salk_128719C) mutants are in the Columbia-0 (Col-0) background. Wild-type Col-0 and mutants seeds were surface sterilized, rinsed with sterile water, and stratified at 4 °C for at least 2 days. Then, seeds were germinated and grown on 1/2 Murashige and Skoog agar plates (half-strength Murashige and Skoog salts, 1% sucrose, 0.8% agar, and pH 5.7) in a growth cabinet at 22 °C under a 16-h light/8-h dark photoperiod. For real-time RT-PCR analysis, 5-day-old seedlings were homogenized, and total RNA was extracted using RNeasy Plant mini kit (Qiagen). The cDNA was synthesized from 500 ng of total RNA with a Transcriptor First Strand cDNA Synthesis Kit (Roche Applied Science) according to the manufacturer's instructions. The TaqMan-based real-time RT-PCR analysis was carried out in a real-time LightCycler 480 PCR system (Roche Applied Sci-

[3] K. Nemoto, N. Takemori, M. Seki, K. Shinozaki, and T. Sawasaki, unpublished data.

ence) using LightCycler 480 Probes Master (Roche Applied Science) and Universal ProbeLibrary (Roche Applied Science), and using *ACTIN4* (At5g59370) (forward primer 5′-TACGGCTTTGGCTCCAAGTA-3′; reverse primer 5′-CTGCTTTCGCAATCCACAT-3′; probe number 55) as the control gene. We used the following primer pairs and Universal ProbeLibrary selected by Assay Design Center program: *CRK1* (At2g41140) (forward primer 5′-CGTGACCTTAAACCCGAGAAC-3′; reverse primer 5′-GCTTGACATAGTCAGAAAGACCAA-3′; probe number 82), *CRK2* (At3g19100) (forward primer 5′-TATGATGCGTTCGAGGACAA-3′; reverse primer 5′-AGAGTATTTTCCTCCCCTTGCT-3′; probe number 10), *CRK3* (At2g46700) (forward primer 5′-ATGTGAGGACGCCAATAACG-3′; reverse primer 5′-GGGTATTTACCACCCCTTGC-3′; probe number 22), *CRK4* (At5g24430) (forward primer 5′-TGAGGATGCTGATAATGTCTTTGT-3′; reverse primer 5′-CAGGGTATCGTCCACCTCTC-3′; probe number 39), *CRK5* (At3g50530) (forward primer 5′-TTCCTCATTTCTATGATGCTTATGA-3′; reverse primer 5′-TGTGTACTTCCCACCTCTTGAA-3′; probe number 63), *CRK6* (At3g49370) (forward primer 5′-GGATTCGGATAATGTCTTTGTTG-3′; reverse primer 5′-GACCACCTCTCGCCAAAATA-3′; probe number 39), *CRK7* (At3g56760) (forward primer 5′-TGCTCTGCTAAGGGGAAAAA-3′; reverse primer 5′-TGCAATTGCCGTAGTCATCT-3′; probe number 5), *CRK8* (At1g49580) (forward primer 5′-CCCAGAGTTTCTTGCTTTGC-3′; reverse primer 5′-AGCTGCACAAAACTCTTCAAAA-3′; probe number 6).

For Tyr phosphorylation analysis of endogenous TBBs, 14-day-old seedlings were homogenized in the cell lysis buffer and cleared by centrifugation at 12,000 × *g* for 10 min. Immunoprecipitation, Phos-Tag SDS-PAGE, and immunoblot analysis were carried out as described above.

Results

Identification of Tyr Autophosphorylation Protein Kinases Using a Wheat Cell-free Protein Array—Autophosphorylation of PKs is an important aspect of regulatory systems such as activation or inactivation by the autophosphorylation-dependent conformational change (26). Many biochemical analyses demonstrate that almost all PKs catalyze intra/inter-molecular autophosphorylation reactions (27). Actually, in our previous report, many *Arabidopsis* PKs showed the Ser/Thr autophosphorylation activity (17). These findings prompt us to propose that Tyr-autophosphorylation activity might be a useful clue to identify plant PK(s) for Tyr phosphorylation. To search for *Arabidopsis* PKs for Tyr phosphorylation, we therefore profiled Tyr-autophosphorylation activity using a wheat cell-free based luminescent method with anti-phospho-Tyr (Tyr(P)) antibody in this study (Fig. 1*A*). In our previous study, more than half of the PKs that showed four times stronger luminescent signal than background had indeed the high Ser/Thr autophosphorylation activity (17). Thus, we concluded that these PKs are more likely to have autophosphorylation activity. Based on this threshold, 89 of 759 PKs were considered candidates for Tyr-autophosphorylation activity by autophosphorylation profiling (supplemental Table S1). Furthermore, to further enrich PKs having the high Tyr-autophosphorylation activity, profiling data of the Tyr-autophosphorylation activity was compared with our previous Ser/Thr-autophosphorylation data (Fig. 1*B*). Finally, we selected 38 Tyr-autophosphorylation PK candidates that showed 4-fold stronger luminescence with anti-Tyr(P) antibody than with anti-Ser(P)/Thr(P) antibody (Tyr(P)/Ser(P)-Thr(P)) (Table 1). However, we cannot conclude that these PKs have high Tyr-autophosphorylation activity based on antibody detection alone as the signal value is correlated to the number of phosphorylated molecules and phosphorylation site. Furthermore, the effects of the three-dimensional structure of the PK on the accessibility and specificity of the antibodies cannot be discounted. Unfortunately, the affinity and specificity of currently available anti-Ser(P)/Thr(P) antibodies are lower than those of anti-Tyr(P) antibodies. Thus, currently available anti-Ser(P)/Thr(P) antibodies are almost certainly unable to solve these problems because of their low specificity. Nevertheless, at present, an approach to compare the luminescent signal would be probably effective as an indicator for high-throughput autophosphorylation profiling of PKs.

To confirm Tyr autophosphorylation, we performed phosphoamino acid analysis and dephosphorylation assays. By TLC, 22 of the 25 tested PKs showed phosphorylation of the Tyr residue (Fig. 1*C*). A phospho-Tyr residue was difficult to detect in the other 3 PKs (PK-B11, -C05, and -C06 in Fig. 1*C*). This might be due to the differences in PK kinetic properties. Another explanation for this might be that they are not able to autophosphorylate further because the autophosphorylation levels of these PKs had been saturated during the *in vitro* translation. However, the Tyr-autophosphorylation signal of all 38 PKs as observed decrease by incubation with AtPTP1 (Fig. 1*D*). These results suggest that these 38 PKs have Tyr-autophosphorylation activity (Table 1). Next, we randomly selected PK-A09, -B01, -B08, -B12, -C02, and -D01, and tested whether these PKs have re-autophosphorylation activity. Expectedly, all tested PKs showed activity after dephosphorylation by treatment with λ-protein phosphatase (Fig. 1*E*). In addition, we randomly selected PK-A01, -A11, -B01, -B07, -B10, and -D01, and generated K_D proteins by mutating conserved Lys residues in the ATP binding sites to Arg. All the mutated PKs failed to react with anti-Tyr(P) antibody (Fig. 1*F*). Taken together, these results suggest that Tyr phosphorylation in PKs is due to the kinase activity itself. According to the PlantsP classification, these 38 PKs are mainly classified into five groups: GSK3/Shaggy-like PK (8 clones), MAPK (6 clones), RLK/RLCK (8 clones), casein kinase I/casein kinase I-like (CK1/CKL) (4 clones), and CRK (3 clones). Because the Tyr-autophosphorylation activity of some of the PKs classified within the GSK3/Shaggy-like PK, MAPK, RLK/RLCK, and CK1/CKL families has been identified in previous studies (14, 28), suggesting that this approach is able to find PKs having the Tyr-autophosphorylation activity.

On the other hand, the CRK family, which was classified as part of the Ser/Thr-type CDPK-sucrose non-fermenting-1-related PK superfamily (29), has not been previously characterized. In the profiling data, three CRKs showed Tyr-autophosphorylation activity. This finding supports the suggestion that CRKs probably has Tyr-autophosphorylation activity and we focused on the analysis of the biochemical properties of CRKs. To confirm the Tyr-autophosphorylation sites of CRK3, we predicted phosphorylation sites using a web page based pro-

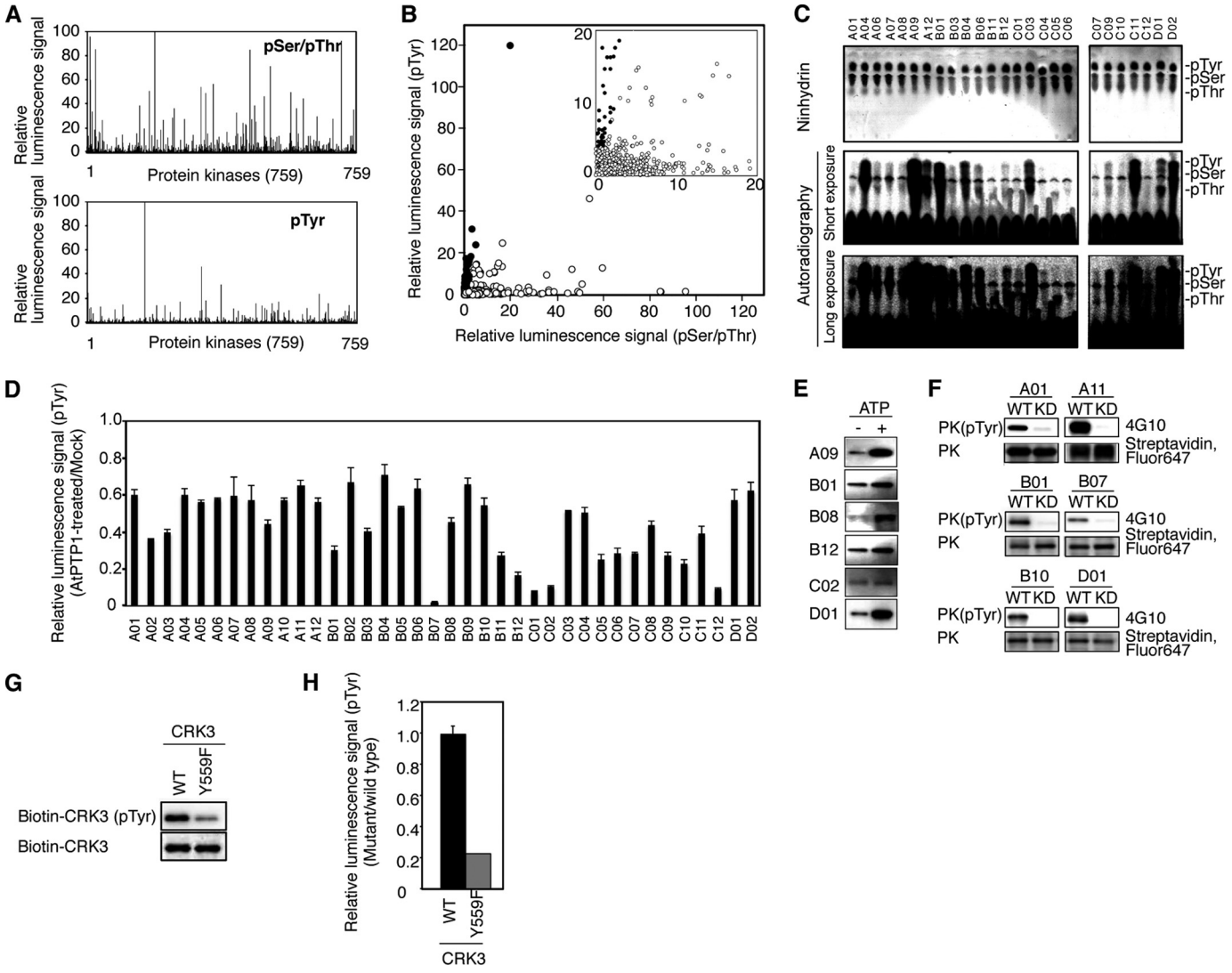

FIGURE 1. **Screening of Tyr-autophosphorylation PKs using a wheat cell-free based protein array.** *A,* autophosphorylation analysis of 759 biotinylated PKs using a luminescent system with anti-Ser(P)/Thr(P) or anti-Tyr(P) antibodies. All data represent the average of two independent experiments and the background for each experiment was controlled using the relevant non-biotinylated PK. *B*, relative luminescent signals between anti-Ser(P)/Thr(P) (*horizontal axis*) and anti-Tyr(P) antibody (4G10) (*vertical axis*). *Black circles* represent PKs that are more reactive with anti-Tyr(P) antibody than with anti-Ser(P)/Thr(P) antibody. *C,* phosphoamino acid analysis. Phospho-Tyr (*pTyr*), phospho-Ser (*pSer*), and phospho-Thr (*pThr*) in PKs were confirmed by one-dimensional TLC with [γ-^{32}P]ATP. The ninhydrin panel shows the location of standard Tyr(P), Ser(P), and Thr(P) (*upper*). The autoradiography panel shows ^{32}P-labeled Tyr(P), Ser(P), and Thr(P) (*middle*: short exposure and bottom long exposure). *D*, the dephosphorylation assay of 38 PKs by AtPTP1 using a luminescent system with anti-Tyr(P) antibody. All data represent the average of three independent experiments and dephosphorylation efficiency was defined as the ratio between PTP1-treated kinases and untreated ones. *E*, Tyr autophosphorylation of PKs was confirmed by immunoblotting with anti-Tyr(P) antibody (4G10) with or without ATP. *F*, *in vitro* autophosphorylation assay using WT or K_D mutants. Biotinylated PKs were detected using Fluor 647 strepavidin. *G, in vitro* autophosphorylation assay of autophosphorylation site mutants. Wild-type biotinylated CRK3 and CRK3^{Y559F} mutants were used. *H,* autophosphorylation analysis of CRK3 by a luminescent system. The data presented are the average of three independent experiments. *Black* and *gray bars* represent wild-type CRK3 and autophosphorylation site mutants, respectively.

gram (PhosPhAt, NetPhos 2.0). Following this, the predicted Tyr^{559} residue sites were changed to Phe and the Tyr^{559}-Phe (Y559F) mutant was used for *in vitro* kinase assays. Immunoblot analysis showed that autophosphorylation was decreased in CRK3-Y559F (Fig. 1*G*). Similarly to immunoblotting, luminescent analysis showed that the Tyr-autophosphorylation signal of CRK3-Y559F decreased by 80% in comparison with that of the wild-type (Fig. 1*H*). The CRK3-autophosphorylation site was also analyzed by MS analysis and phospho-Tyr^{559} was detected (supplemental Table S2).

Substrate Screening of CRK3 by Pulldown Assay Based on a Wheat Cell-free System—To better understand the biochemical properties of CRKs, we selected CRK3 and explored the substrate proteins that Tyr residue(s) are phosphorylated by CRK3. Protein extracts from *Arabidopsis* cultured cells were used for pulldown assays with recombinant biotin-labeled CRK3 and anti-Tyr(P) antibody was used to detect Tyr phosphorylation. Some Tyr-phosphorylated proteins interacting with CRK3 were detected (Fig. 2*A*) and, subsequently, Coomassie Brilliant Blue-stained bands of ~50 kDa molecular mass showing Tyr phosphorylation were analyzed using MS. These proteins identified TBB2, TBB7, and TBB9 (supplemental Table S3).

To confirm whether the TBBs are substrate proteins of CRK3 for Tyr phosphorylation, these three TBB proteins were used for *in vitro* kinase assays. We also tested whether CRK2 and CRK8 could phosphorylate these three TBB proteins because

TABLE 1
List of Tyr autophosphorylation protein kinases

Tyr autophosphorylation PK No.	AGI code	Gene name	Relative value[a]			PPA[b]	PlantP family[c]
			Ser(P)-Thr(P)	Tyr(P)	Tyr(P)/Ser(P)-Thr(P)		
A01	At5g15080		3.4	31.8	9.4	+	Family 1.2.2- receptor-like cytoplasmic kinase VII
A02	At4g34440		0.8	17.6	21.8	NT	Family 1.6.2-plant external response-like kinase
A03	At1g55200		0.8	5.6	6.7	NT	Family 1.6.2- plant external response-like kinase
A04	At3g24550		0.7	4.8	6.6	+	Family 1.6.2-plant external response-like kinase
A05	At5g56790		5.0	24.1	4.8	NT	Family 1.6.2-plant external response-like kinase
A06	At1g70520		1.1	14.7	13.9	+	Family 1.7.2-DUF26 kinase
A07	At2g26330	*ERECTA*	1.8	8.7	4.8	+	Family 1.12.4-leucine-rich repeat kinase XI and XII
A08	At1g48480	*RKL1*	19.9	120.1	6.0	+	Family 1.13.3-leucine-rich repeat kinase III
A09	At4g28880	*CKL3*	0.4	9.0	25.1	+	Family 3.1.1-casein kinase I family
A10	At4g28540	*CKL6*	1.1	8.1	7.7	NT	Family 3.1.1-casein kinase I family
A11	At4g28860	*CKL4*	2.2	16.4	7.6	NT	Family 3.1.1-casein kinase I family
A12	At5g43320	*CKL8*	2.2	9.2	4.1	+	Family 3.1.1-casein kinase I family
B01	At1g73500	*MKK9*	0.4	7.6	19.9	+	Family 4.1.3-MAP2K
B02	At3g61960		0.9	4.2	4.6	NT	Family 4.1.7-APG1-like kinase
B03	At1g49580	*CRK8*	0.6	4.4	7.0	+	Family 4.2.1-calcium dependent PK
B04	At2g46700	*CRK3*	1.8	9.4	5.3	+	Family 4.2.1-calcium dependent PK
B05	At3g19100	*CRK2*	0.9	4.3	4.8	NT	Family 4.2.1-calcium dependent PK
B06	At3g10540		1.0	4.7	4.8	+	Family 4.2.6-IRE/NPH/PI-dependent/S6 kinase
B07	At2g30040	*MAPKKK14*	2.4	17.6	7.3	NT	Family 4.4.1-unknown function kinase
B08	At3g45640	*MPK03*	0.2	5.8	27.4	NT	Family 4.5.1-MAPK family
B09	At4g01370	*MPK04*	0.3	4.1	14.2	NT	Family 4.5.1-MAPK family
B10	At2g43790	*MPK06*	0.6	4.4	8.0	NT	Family 4.5.1-MAPK family
B11	At4g19110		2.9	18.6	6.4	ND	Family 4.5.1-MAPK family
B12	At1g59580	*MPK02*	0.8	4.6	5.9	+	Family 4.5.1-MAPK family
C01	At2g01450	*MPK17*	1.1	5.9	5.5	+	Family 4.5.1-MAPK family
C02	At5g39420		0.3	5.9	19.8	NT	Family 4.5.2-CDC2-like kinase family
C03	At1g03740		0.9	5.3	5.9	+	Family 4.5.2-CDC2-like kinase family
C04	At4g18710	*BIN2/ASKη*	0.3	4.7	15.7	+	Family 4.5.4-GSK3/Shaggy-like PK Family
C05	At3g61160	*ASKβ*	0.4	6.4	14.1	ND	Family 4.5.4-GSK3/Shaggy-like PK Family
C06	At4g00720	*ASKθ*	0.9	12.4	13.2	ND	Family 4.5.4-GSK3/Shaggy-like PK family
C07	At1g57870	*ASKδ/AtSK42*	1.4	16.3	12.0	+	Family 4.5.4-GSK3/Shaggy-like PK family
C08	At1g06390	*AtGSK1/ASKι*	1.1	11.4	10.4	NT	Family 4.5.4-GSK3/Shaggy-like PK family
C09	At2g30980	*ASKdζ*	1.8	14.7	8.2	+	Family 4.5.4-GSK3/Shaggy-like PK family
C10	At5g26750	*AtSK11/ASKα*	0.7	5.3	7.6	+	Family 4.5.4-GSK3/Shaggy-like PK family
C11	At3g05840	*AtSK12/ASKγ*	0.8	6.3	7.5	+	Family 4.5.4-GSK3/Shaggy-like PK family
C12	At2g40120		1.8	7.4	4.1	+	Family 4.5.8-unknown function kinase
D01	At4g28980	*CDKF;1*	1.8	16.3	8.8	+	−
D02	At5g58350		1.1	6.5	6.1	+	−

[a] Ser(P)-Thr(P) and Tyr(P) are the relative values of the non-biotinylated PKs. All data represent the average of two independent experiments and the background was controlled for each experiment using the relevant non-biotinylated PK.
[b] Results of phosphoamino acid analyses (PPA). +, Tyr(P) residue was detected; ND, not detected; NT, not tested.
[c] The classification is based on the PlantP database. −, not annotated.

CRK2 and CRK8 also showed Tyr-autophosphorylation activity. Our results show that the three CRK proteins tested can phosphorylate TBB2 and TBB7 at the Tyr residue but not TBB9 (Fig. 2*B*). Comparison of amino acid sequences showed that TBB2 and TBB7 have an extra C-terminal region including Tyr residue(s) (Fig. 2*C*), whereas TBB9 is missing this region. By mutation of the Tyr residue to Phe (Y443F or Y449F), Tyr phosphorylation of TBB7 was decreased (Fig. 2*D*), suggesting that the two Tyr residues are major phosphorylation sites for CRK2, CRK3, and CRK8. Interestingly, Tyr phosphorylation of β-tubulins in *Arabidopsis* and tobacco plants has already been reported (12, 30, 31). Our finding suggests that the three CRKs are the responsible PKs for Tyr phosphorylation of β-tubulins.

Substrate Screening of CRK2 and CRK3 by PPI Assay Using TFs Array—We found only two TBB substrate proteins by pulldown assays using cell extracts. Thus, we used a protein array of *Arabidopsis* TFs as previously described (18) to explore more substrate proteins phosphorylated at the Tyr residue(s) by CRK2 and CRK3. From the 647 TFs in the protein array, we selected 188 TFs characterized in previously published papers (supplemental Table S4). To identify substrate proteins for Tyr phosphorylation, we adopted a two-step screening procedure: 1) PPI between CRK2 or CRK3, and TFs using a luminescent method (Fig. 3*A* and supplemental Table S4), and 2) *in vitro* Tyr-phosphorylation assay using the top 20 proteins that showed the strongest PPI assay signals. After this double screening, four TFs, ethylene response factor 13 (ERF13) (At2g44840), WRKY DNA-binding protein 14 (WRKY14) (At1g30650), ERF subfamily B-4 of ERF/AP2 transcription factor 2.6 (RAP2.6) (at1g43160), and cryptochrome-interacting basic helix-loop-helix 5 (CIB5) (At1g26260), were found to be Tyr phosphorylation substrates of CRK2 or CRK3 (Fig. 3*B* and Table 2). Because ERF13 and WRKY14 were phosphorylated by both CRK2 and CRK3, they were used for further analysis. Tyr phosphorylation of the two substrates was not detected when K_D forms of CRK2 and CRK3 were used, indicating that ERF13 and WRKY14 were phosphorylated by CRK2 and CRK3 in an activity-dependent manner (Fig. 3*C*). In summary, we identified a total of six substrate Tyr-phosphorylated proteins *in vitro* by CRK2, CRK3, and CRK8 using pulldown and PPI assays (Table 2).

CRK Family Has Tyr Phosphorylation Activity—Next, we analyzed the biochemical properties of CRK2 and CRK3 by using ERF13 as a substrate. First, we analyzed whether CRK2 and CRK3 phosphorylate not only Tyr but also Ser/Thr residues. AtPTP1 is known to be a Tyr-specific protein phospha-

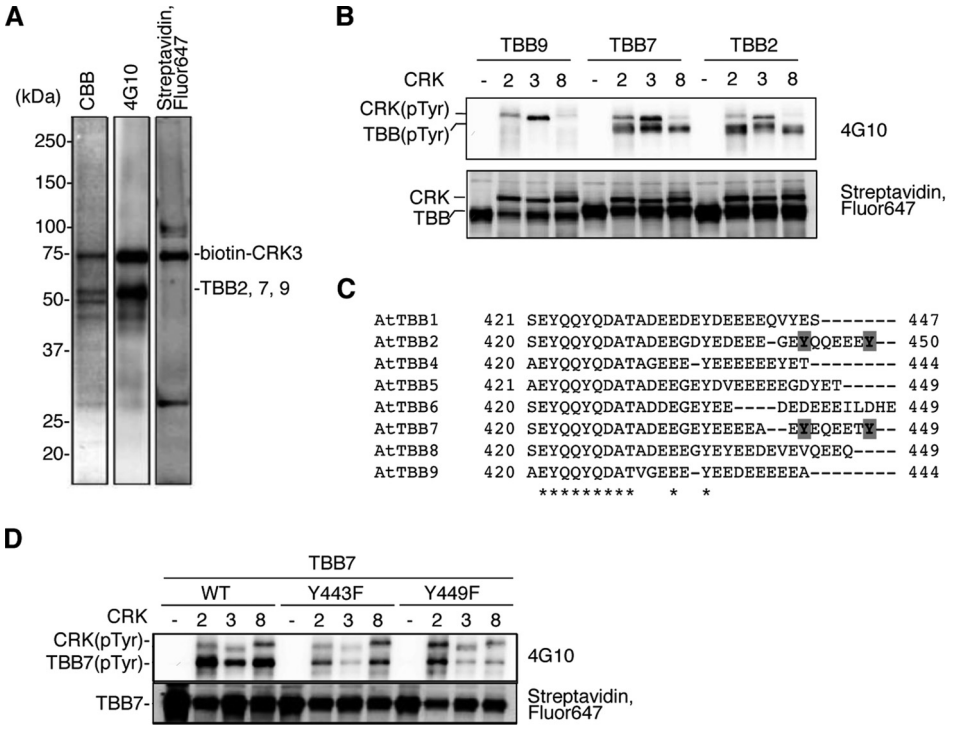

FIGURE 2. **CRK2, CRK3, and CRK8 could phosphorylate C-terminal Tyr residues of TBB2 and TBB7.** *A*, affinity purified Tyr phosphorylation proteins interacting with biotinylated CRK3 (biotin-CRK3) from *Arabidopsis* cell lysates. *B*, *in vitro* kinase assay of biotinylated CRK2, CRK3, and CRK8 with biotinylated TBB2, TBB7, and TBB9. *C*, alignment of Tyr phosphorylation sites sequences of *Arabidopsis* TBBs. Multiple alignment of the C-terminal of TBBs was performed using the ClustalW program (DNA Data Bank of Japan). The phosphorylation sites identified by mutant analysis are highlighted in *gray*. Identical amino acids among AtTBB1 (At1g75780), AtTBB2 (At5g62690), AtTBB4 (At5g44340), AtTBB5 (At1g20010), AtTBB6 (At5g12250), AtTBB7 (At2g29550), AtTBB8 (At5g23860), and AtTBB9 (At4g20890) are marked with *asterisks*. *D*, *in vitro* kinase assay of biotinylated CRK2/3/8 with biotinylated TBB7 mutants (Y443F and Y449F). Tyr-phosphorylated residue (*pTyr*) was detected by anti-Tyr(P) antibody (4G10) and the amount of protein loaded was determined by CBB stain or Fluor 647 strepavidin (*A*, *B*, and *D*). *CBB*, Coomassie Brilliant Blue.

tase (4, 23). A dephosphorylation assay revealed that both CRK2-dependent and CRK3-dependent phosphorylations of ERF13 dramatically were decreased upon treatment with AtPTP1 (Fig. 3*D*). Furthermore, AtPTP1 significantly dephosphorylated even radioisotopically CRK-phosphorylated ERF13 proteins (Fig. 3*E*). In another approach, Tyr residue(s) were mutated to Phe (Fig. 3*F*). A significant decrease in Tyr phosphorylation was observed in Tyr^{16}-Phe (Y16F) and Tyr^{207}-Phe (Y207F) mutants (Fig. 3*F*), whereas the $Tyr^{16/207}$-Phe (Y16F/Y207F) double mutation completely lost Tyr phosphorylation (Fig. 3*G*). These mutation analyses revealed that Tyr^{16} and Tyr^{207} residues are the main phosphorylation sites in ERF13.

The *Arabidopsis* genome contains eight *CRK* genes (Fig. 3*H*). To test the activity of other CRKs, we synthesized five CRKs and analyzed their Tyr-auto- and trans-phosphorylation activity. All CRKs exhibited Tyr-autophosphorylation activity, and particularly CRK2, CRK3, and CRK4 showed high activity (Fig. 3*I*). In addition, five CRKs could phosphorylate ERF13 (Fig. 3*I*), even though the degree of Tyr ERF13 phosphorylation differed. CRK2 and CRK3 showed the highest kinase activity, using ERF13 protein as a substrate, when compared with the other CRKs. Furthermore, we searched for the *CRK3* orthologous gene in soybean and found Glyma07g05750 (74% similarity to *AtCRK3*), which we named *GmCRK3* (Fig. 3*H*). The cDNA was cloned from soybean seedlings and GmCRK3 protein was synthesized using the cell-free system. *In vitro* kinase assay revealed that GmCRK3 also phosphorylated *Arabidopsis* ERF13 (Fig. 3*J*), indicating that GmCRK3 has PTK activity.

Overexpression of CRK2 and CRK3 Could Phosphorylate Exogenous ERF13 and Endogenous β-Tubulin in Cultured Cells—To confirm the Tyr phosphorylation activity of CRK2 and CRK3 in cells, we used cultured *Arabidopsis* cells. First, we investigated the cellular localization of these proteins. Transient expression analyses revealed that CRK3-YFP and ERF13-GFP are partially localized in the nucleus of cultured cells. CRK2-YFP is likely to localize to the plasma membrane as well as to the nucleus to a lesser degree (Fig. 4*A*). Similar results were observed in onion epidermal cells transiently expressing CRK3-GFP (32). Next, we expressed CRK2 or CRK3 together with ERF13 in cells. Immunoprecipitation with anti-GFP followed by immunoblot analysis with antibody to phosphorylated Tyr showed that CRK3WT phosphorylated ERF13-GFP, whereas CRK2WT did not (Fig. 4*B*), and ERF13Y16F/Y207F-GFP was not phosphorylated by CRK3WT. Because expression of K_D forms of CRK2 and CRK3 was very low in cells compared with wild-type forms, we failed to analyze K_D forms (Fig. 4*B*). Taken together, these results suggest that CRK3, instead of CRK2, phosphorylates the Tyr^{16} and Tyr^{207} sites of ERF13 in cells. In addition, we tried to investigate the Tyr phosphorylation of endogenous TBBs. Because Tyr phosphorylation of TBBs was very weak, we used an immunoprecipitation method with anti-TBB antibody to increase the detection sensitivity. A phosphoprotein mobility shift assay with Phos-tag acrylamide (33) was used because the immunoprecipitated TBBs could not be detected on normal SDS-PAGE gel incubated with heavy chain anti-TBB antibody. Due to the covalent modification of the phosphory-

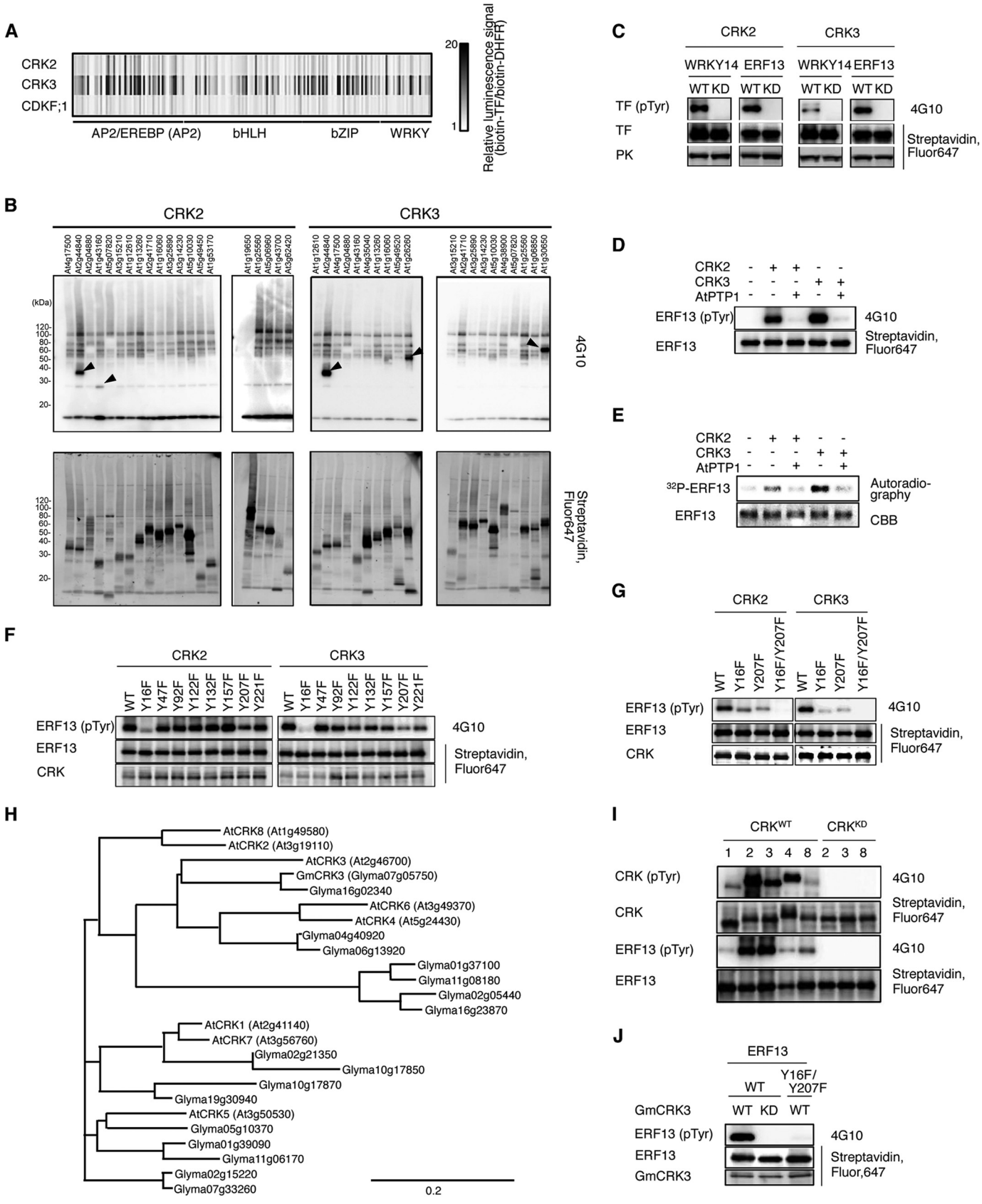
A
CRK2
CRK3
CDKF;1
AP2/EREBP (AP2)
bHLH
bZIP
WRKY
20
1
Relative luminescence signal (biotin-TF/biotin-DHFR)
B
CRK2
CRK3
(kDa)
120-
100-
80-
60-
50-
40-
30-
20-
4G10
Streptavidin, Fluor647
C
CRK2
CRK3
WRKY14
ERF13
WT KD
TF (pTyr)
TF
PK
4G10
Streptavidin, Fluor647
D
CRK2
CRK3
AtPTP1
ERF13 (pTyr)
ERF13
4G10
Streptavidin, Fluor647
E
CRK2
CRK3
AtPTP1
32P-ERF13
ERF13
Autoradio-graphy
CBB
F
CRK2
CRK3
WT
Y16F
Y47F
Y92F
Y122F
Y132F
Y157F
Y207F
Y221F
ERF13 (pTyr)
ERF13
CRK
4G10
Streptavidin, Fluor647
G
CRK2
CRK3
WT
Y16F
Y207F
Y16F/Y207F
ERF13 (pTyr)
ERF13
CRK
4G10
Streptavidin, Fluor647
H
AtCRK8 (At1g49580)
AtCRK2 (At3g19110)
AtCRK3 (At2g46700)
GmCRK3 (Glyma07g05750)
Glyma16g02340
AtCRK6 (At3g49370)
AtCRK4 (At5g24430)
Glyma04g40920
Glyma06g13920
Glyma01g37100
Glyma11g08180
Glyma02g05440
Glyma16g23870
AtCRK1 (At2g41140)
AtCRK7 (At3g56760)
Glyma02g21350
Glyma10g17850
Glyma10g17870
Glyma19g30940
AtCRK5 (At3g50530)
Glyma05g10370
Glyma01g39090
Glyma11g06170
Glyma02g15220
Glyma07g33260
0.2
I
CRKWT
CRKKD
1 2 3 4 8 2 3 8
CRK (pTyr)
CRK
ERF13 (pTyr)
ERF13
4G10
Streptavidin, Fluor647
J
ERF13
WT
Y16F/ Y207F
GmCRK3
WT KD WT
ERF13 (pTyr)
ERF13
GmCRK3
4G10
Streptavidin, Fluor,647

TABLE 2
Tyr-phosphorylated proteins as substrates for CRKs

Tyr-phosphorylated substrate protein			CRKs	Method
AGI code	Name	Tyr phosphorylation site		
At5g62690	TBB2		CRK2, CRK3, CRK8	PD[a]
At2g29550	TBB7	Tyr^{443}, Tyr^{449}	CRK2, CRK3, CRK8	PD
At2g44840	ERF13	Tyr^{16}, Tyr^{207}	CRK1, CRK2, CRK3, CRK4, CRK8, GmCRK3[c]	PPI[b]
At1g43160	RAP2.6		CRK2	PPI
At1g26260	CIB5		CRK3	PPI
At1g30650	WRKY14		CRK3	PPI

[a] PD, pull-down.
[b] PPI, protein-protein interaction analysis by AlphaScreen.
[c] *G. max* (soybean).

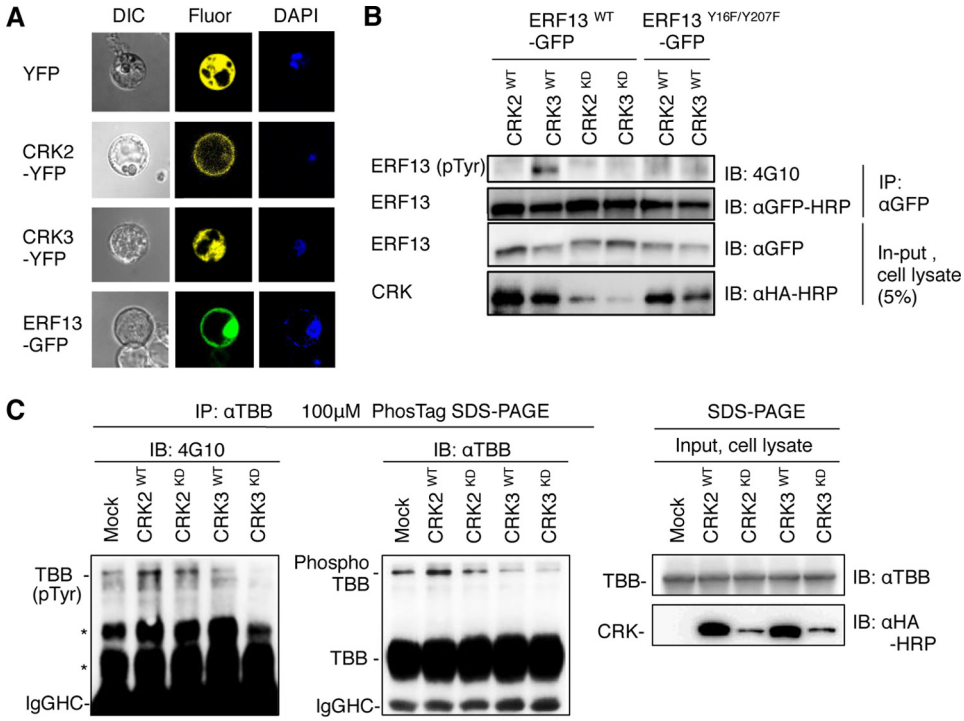

FIGURE 4. **Functional analysis of CRK2 and CRK3 Tyr phosphorylation in cells.** *A*, localizations of CRK2-YFP, CRK3-YFP, and ERF13-GFP in *Arabidopsis* protoplasts. *DIC*, differential interference contrast microscopy; *YFP*, YFP fluorescence; *DAPI*, 4′,6-diamidino-2-phenylindole. *B*, Tyr phosphorylation analysis of ERF13-GFP by protoplast transient expression assays. ERF13-GFP or $ERF13^{Y16F/Y207F}$-GFP was immunoprecipitated with anti-GFP antibody from protoplast lysates. Tyr phosphorylation was detected by anti-Tyr(P) antibody (4G10). Expressions of the WT or K_D forms of CRK2-HA and CRKK3-HA were detected by anti-HA antibody. *C*, Tyr phosphorylation analysis of endogenous TBBs in CRK2 or CRK3 expressing protoplasts. Endogenous TBBs were immunoprecipitated with anti-TBB antibody (*IP: αTBB*) from protoplast lysates, and analyzed using 100 μM Phos-tag acrylamide gel and immunoblotting (*IB*) with 4G10 (*IB: 4G10*) (*left panel*) or anti-TBB antibodies (*IB: αTBB*) (*middle panel*). TBB proteins from 5% of the protoplast lysates were immunopurified and detected by anti-TBB antibody (*Input, cell lysate*) (*left panel*). *pTyr*, phospho-Tyr.

lated TBB by the Phos-tag reagent, a band of low mobility was detected (phospho-TBB in Fig. 4*C*). Following this, Tyr phosphorylation of the TBBs was detected by anti-Tyr antibody 4G10 (shown as *TBB*(*pY*) in Fig. 4*C*). A low level of Tyr phosphorylation of endogenous TBBs was observed in control cells (*Mock* lane), indicating that the Tyr residue of endogenous TBBs is slightly phosphorylated as shown by a previous report (31). Overexpression of CRK2WT induced Tyr phosphoryla-

FIGURE 3. **Substrate identification of CRKs, and biochemical characterization of CRK2 and CRK3.** *A*, heat map of the PPI relative AlphaScreen signals between 188 biotinylated TFs and FLAG-CRK2, FLAG-CRK3, or FLAG-cyclin-dependent kinase F;1 (*CDKF;1*). All data represent the average of two independent experiments and the background was controlled using dihydrofolate reductase (*DHFR*) from *E. coli*. *B*, *in vitro* Tyr phosphorylation assay using the top 20 proteins of interacting clones. After the incubation of FLAG-CRK2 or FLAG-CRK3, and biotinylated TF, Tyr phosphorylation was detected by immunoblot analysis with anti-Tyr(P) antibody (4G10) (*upper panel*). Biotinylated proteins were detected by Fluor 647 streptavidin (*lower panel*). *Black arrowhead* indicates the Tyr phosphorylation signal. *C*, *in vitro* kinase assay of WT or K_D form of biotinylated CRK2 or CRK3 with biotinylated substrates. *D* and *E*, *in vitro* AtPTP1 dephosphorylation assay of biotinylated ERF13 phosphorylated by FLAG-CRK2 and FLAG-CRK3. Phosphorylation was detected by anti-Tyr(P) antibody (4G10) (*D*) or autoradiography using [γ-^{32}P]ATP (*E*). *F* and *G*, *in vitro* kinase assay of CRK2 and CRK3 with wild-type ERF13 and its Phe mutants. Eight Tyr residues were mutated to Phe in ERF13 (Y16F, Y47F, Y92F, Y122F, Y132F, Y157F, Y207F, and Y221F) and used for *in vitro* kinase assays (*F*). *In vitro* CRK2 and CRK3 phosphorylation site(s) of ERF13 were analyzed using its mutants (Y16F, Y207F, and Y16F/Y207F) (*G*). *H*, phylogenetic tree showing the sequence relationships between CRK proteins from *Arabidopsis* and *Glycine max* (soybean). The amino acid sequences of the *Arabidopsis* CRK family were retrieved from the TAIR and GreenPhyl databases. The amino acid sequences for the soybean homolog of *Arabidopsis* CRK were retrieved by BLAST searches against the Phytozome and GreenPhyl databases. A phylogenetic tree was constructed using ClustalW and the Neighbor joining (NJ) method using the tools of the DDBJ program. The *scale bar* indicates 0.2 substitutions per amino acid. *I* and *J*, *in vitro* kinase assay of the CRK family. Five wild-type *Arabidopsis*-biotinylated CRKs (1–4 and 8), K_D-biotinylated CRKs (2, 3, and 8) (*I*), and soybean GmCRK3 (*J*) were used for *in vitro* kinase assay with biotinylated ERF13. Tyr-phosphorylated (*pTyr*) protein was detected by anti-Tyr(P) antibody (4G10) and the amount of protein loaded was determined by Coomassie Brilliant Blue (*CBB*) stain or Fluor 647 strepavidin (*B-G* and *I-J*).

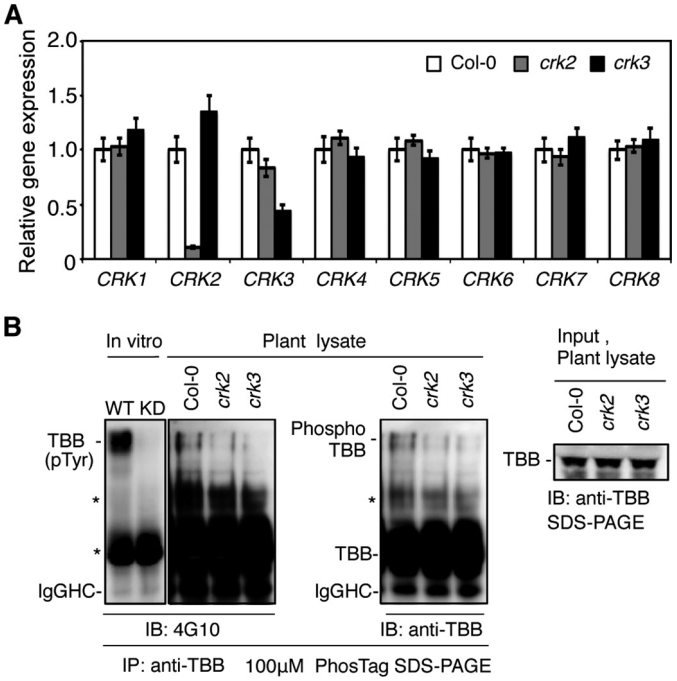

FIGURE 5. **Tyr phosphorylation of endogenous TBBs was decreased in *crk2* and *crk3* mutants.** *A*, analysis of *CRK* family gene expression in *crk2* and *crk3* by real-time RT-PCR. Data are expressed as relative values normalized by the value of wild-type Col-0 plants. All data represent averages ($n = 3$, ± S.D.). *B,* Tyr phosphorylation analysis of endogenous TBBs in Col-0, *crk2*, or *crk3* mutants. Endogenous TBBs were immunoprecipitated from protein lysates using anti-TBB antibodies (*IP: αTBB*), and analyzed using 100 μM Phos-tag acrylamide gel and immunoblotting (*Plant lysate*) (*left* and *middle panel*). Tyr-phosphorylated proteins or TBBs were detected by anti-Tyr(P) (*IB: 4G10*) (*left*) or anti-TBB antibodies (*IB: αTBB*) (*middle* and *right panel*). Five percent of the input lysates were analyzed by anti-TBB antibody (*Input, Plant lysate*). Tyr-phosphorylated recombinant TBB7 was analyzed by a similar method (*in vitro*). *IgGHC*, IgG heavy chains; *pTyr*, phospho-Tyr.

tion of endogenous TBBs ($CRK2^{WT}$ lane), whereas that of CRK3WT did not ($CRK3^{WT}$ lane). These results suggest that CRK2, but not CRK3, phosphorylates endogenous TBB in cultured cells.

Tyr Phosphorylation of TBBs Was Decreased in CRK2- and CRK3-deficient Mutants—To further clarify Tyr phosphorylation of endogenous CRK2 or CRK3 in plants, the Tyr phosphorylation level of TBBs in CRK2- and CRK3-deficient mutants (*crk2* and *crk3* respectively) was analyzed. *CRK2* gene expression dramatically decreased in the *crk2* mutant (Fig. 5*A*). The *CRK3* gene expression level in the *crk3* mutant was 50% lower than that in the Col-0 wild-type. Protein levels of the endogenous TBBs were almost the same as in wild-type plants (*right panel* in Fig. 5*B*). Using the phosphoprotein mobility shift assay, we observed that Tyr phosphorylation levels of endogenous TBBs were lower in *crk2* and *crk3* mutants than in wild-type plants (*left panel* in Fig. 5*B*). This result suggests that in *Arabidopsis* plants, Tyr phosphorylation of TBBs is mainly catalyzed by CRK2 and CRK3. Taken together, these data strongly suggest that *Arabidopsis* CRKs function as PKs for Tyr phosphorylation in plants.

Discussion

In this study, we profiled the autophosphorylation activity of 759 PKs by combining a wheat cell-free system and a high-throughput AlphaScreen method, and identified 38 PKs with Tyr-autophosphorylation activity. The 38 PKs were mainly classified into five groups: GSK3/Shaggy, MAPK, RLK/RLCK, CK1/CKL, and CRK. Like in mammals, several plant MAPKs and GSK3/Shaggy-like kinases have already been reported to show Tyr-autophosphorylation activity (14, 34, 35). Indeed, Tyr phosphorylation sites of most of these PKs have been identified already by MS analysis (6, 36). In mammals, CK1 is a well conserved Ser/Thr-specific PK (37). In our study, four CK1/CLKs showed Tyr-autophosphorylation activity and *Arabidopsis* CKL9 has previously been reported to have a dual-specific kinase activity (28). Therefore, the biochemical properties of CK1/CKLs might be different in plants from those in mammals. Many previous studies have suggested that several RLK/RLCKs such as BRASSINOSTEROID-INSENSITIVE 1 (BRI1) and BRI1-associated kinase 1 (BAK1) have Ser-, Thr-, and Tyr-autophosphorylation activity (38, 39). Our results revealed that the novel eight RLK/RLCKs identified have Tyr-autophosphorylation activity. However, BRI1 and BAK1 did not show a strong Tyr-autophosphorylation signal. The lack of Tyr-autophosphorylation signal in our study might be because full-length BRI1 and BAK1 may require a brassinosteroid ligand and/or BRI1/BAK1-heterodimerization for the activation (40–42) or, alternatively, the three-dimensional structure of the two PKs might disturb the accessibility of the anti-Tyr(P) antibody.

By autophosphorylation profiling and *in vitro* kinase assay, we showed that all tested CRKs, five *Arabidopsis* CRKs, and one soybean GmCRK3 have Tyr-autophosphorylation and trans-phosphorylation activities. A previous study using MS analysis revealed that Tyr phosphorylation was observed at the Tyr^{52} of CRK4 (6). Furthermore, we identified a new Tyr-autophosphorylation site (Tyr^{559}) of CRK3 in addition to the previously reported Ser/Thr-autophosphorylation sites (43). These findings suggest that the CRK family is a novel angiosperm-specific PK family for Tyr phosphorylation. CRK family members have a Ser/Thr kinase domain and a degenerate calcium-binding EF-hand motif, and these structures resemble those found in Ser/Thr-specific CDPKs (29). Previous studies have shown that the kinase activity of *Arabidopsis* CRK1, and rice and tobacco CRKs is enhanced by calcium/calmodulin but that of CRK3 is not (44–49). In this study, CRK2 and CRK3 showed the highest auto/trans-phosphorylation activity among the *Arabidopsis* CRK family members. Similarly to CRK3, CRK2 might not require calcium/calmodulin for activation. The biochemical and biological functions of CDPKs have been well characterized, and these PKs have been shown to play an important role in the signaling pathways of the abscisic acid, stress and metabolic responses (50, 51). Recent studies have shown that CPK16, CPK18, and CPK28, phylogenetically closely related to CRKs, phosphorylated Tyr residues in plants, and CPK28 had Tyr-autophosphorylation activity (5, 15, 16, 36, 52). In addition, Tyr phosphorylation was also observed in other CDPKs. Based on these findings, we conclude that CRKs and several CDPKs might have Tyr-phosphorylation activity.

Previous studies have already shown that the Tyr residues of α- and β-tubulin are phosphorylated in *Arabidopsis* and tobacco, but the phosphorylation site(s) and the kinases responsible for phosphorylation remain unknown (30, 31). By

pulldown assays using protein lysate from cultured cells and *in vitro* kinase assays, we identified the Tyr residues of TBB7 that are phosphorylated by CRK2, CRK3, and CRK8. A cell-based transient assay revealed that CRK2 could phosphorylate Tyr residues of TBBs. Furthermore, Tyr phosphorylation of endogenous TBBs decreased in *crk2* and *crk3* mutants. Our results strongly suggest that CRKs are the responsible kinases for the Tyr phosphorylation of TBBs. Pharmacological approaches showed that PTK and PTP inhibitors can alter the stability and orientation of the microtubules (MTs) (12, 13). In mammals, membrane-associated TBBs were phosphorylated by membrane-associated pp60c-src in nerve growth cones membranes (53). In addition, pp60c-src-dependent Tyr phosphorylation of TBB inhibited the polymerization of MTs (54). However, no significant difference in growth was observed between *crk2* or *crk3*, and wild-type Col-0 plants under normal conditions. This might be because other CRKs might play complementary roles. The role of Tyr phosphorylation of TBBs by CRKs remains unclear. The AtGenExpress global stress expression data set revealed that expression of *CRK2* increased under osmotic stress (55). Thus, CRK2-dependent Tyr phosphorylation might be involved in MT depolymerization or MT orientation maintenance under osmotic stress (56).

In some cases, phosphorylation of TFs can provide a key link between cell signaling and the control of gene expression. By PPI and *in vitro* kinase assays, we identified four Tyr-phosphorylated TFs that are substrate proteins of CRK2 and CRK3. Our approach, which combines a wheat cell-free system and a high-throughput AlphaScreen method, is able to analyze the direct interactions between the PK and the substrate protein with a high sensitivity level, as shown by the previous reports (57, 58). We hypothesized that this approach might be applicable to identify substrate proteins or kinases involved in phosphorylation. By dephosphorylation analysis and mutational analysis of the identified substrate proteins, we showed that CRK2 and CRK3 could phosphorylate ERF13 Tyr residues (Tyr^{16} and Tyr^{207}). In contrast, CRKs-dependent phosphorylation of Ser or Thr residues was hardly observed. These results suggest that CRKs catalyze mainly the trans-phosphorylation of ERF13 Tyr residues. To uncover whether CRK2 and CRK3 can preferentially trans-phosphorylate the Tyr residue of a substrate protein, other substrate proteins would need to be found because it is not possible to clarify the essential biochemical properties of PKs by using pseudosubstrates such as myelin basic protein or peptide. We found only two substrates, ERF13 and TBB7, which Tyr residues were phosphorylated. Thus, we could not confirm whether CRK2 and CRK3 preferentially phosphorylate Ser/Thr or Tyr residues because our data from these two substrate proteins is very limited.

Using a cell-based transient assay, we showed that CRK3 could phosphorylate the Tyr residues (Tyr^{16} and Tyr^{207}) of ERF13-GFP in cells. However, CRK2-dependent Tyr phosphorylation was below the detection limit in this study. Using subcellular localization analysis, we observed that CRK2 was mainly localized to the plasma membrane and slightly to the nucleus. However, cytoplasmic localization might also be possible because we did not compare its localization with a plasma membrane-localized marker protein. Among the CRK family members, six CRKs (1, 2, 3, 5, 7, and 8) were predicted to have a myristoylation/palmitoylation motif in the N terminus (29) and a predicted nuclear localization signal motif was found in all CRKs (59). In fact, tomato CRK1 and CPK/CRK-related tobacco CPK5 that have a myristoylation/palmitoylation motif in the N-terminal are localized to the plasma membrane, whereas motif mutants of these are localized to the nucleus and cytoplasm (60, 61). These findings suggest that CRKs have the potential for nuclear and membrane localization and are able to phosphorylate nuclear and/or membrane proteins.

Previous studies (62) have shown that overexpression of ERF13 causes growth retardation, and increases abscisic acid and glucose sensitivities in *Arabidopsis*. In addition, expression of CRK3 is induced by abscisic acid treatment (53). These findings suggest that Tyr phosphorylation of ERF13 by CRK3 might be involved in the regulation of abscisic acid signaling. However, unfortunately, direct downstream target genes of ERF13 remain unknown. Both CRK3 and CRK2 could phosphorylate WRKY14, and CRK3 phosphorylates CIB5 *in vitro*. Thus, it is possible that both CRK3 and CRK2 play a role in the phosphorylation of these TFs in plants. On the other hand, previous studies have also suggested that some CRKs are involved in the signal transduction of different extracellular stimuli such as salt, low/high-temperature stress, wounding, and phytohormones in *Arabidopsis*, tobacco, tomato, and pea (61, 63–67). Phenome analysis based on genetic techniques might provide significant information regarding the role of CRK-dependent Tyr phosphorylation in plants.

Although many previous studies have strongly suggested the existence of plant PTKs, evidence linking a particular PK to Tyr phosphorylation of substrates *in vivo* has been missing. In this study, we demonstrate that *Arabidopsis* has an angiosperm-specific CRK family involved in Tyr phosphorylation. Furthermore, we have identified six substrate proteins for CRKs. Our results provide the first direct evidence that plant PKs are able to phosphorylate substrate proteins on Tyr residues, and that typical TFs are the target of CRKs as observed in mammals. Furthermore, our data supports the identification of CRKs as the PKs that phosphorylate tubulin *in vivo*. In future studies, the functions of CRKs will be investigated to further clarify the role of Tyr phosphorylation in plants.

Acknowledgments—We thank the Applied Protein Research Laboratory of Ehime University for technical assistance and the Riken BioResource Center for providing Arabidopsis T87 cells.

References

1. Blume-Jensen, P., and Hunter, T. (2001) Oncogenic kinase signaling. *Nature* **411,** 355–365
2. Rudrabhatla, P., Reddy, M. M., and Rajasekharan, R. (2006) Genome-wide analysis and experimentation of plant serine/threonine/tyrosine-specific protein kinases. *Plant Mol. Biol.* **60,** 293–319
3. Goff, S. A., Ricke, D., Lan, T. H., Presting, G., Wang, R., Dunn, M., Glazebrook, J., Sessions, A., Oeller, P., Varma, H., Hadley, D., Hutchison, D., Martin, C., Katagiri, F., Lange, B. M., Moughamer, T., Xia, Y., Budworth, P., Zhong, J., Miguel, T., Paszkowski, U., Zhang, S., Colbert, M., Sun, W. L., Chen, L., Cooper, B., Park, S., Wood, T. C., Mao, L., Quail, P., Wing, R., Dean, R., Yu, Y., Zharkikh, A., Shen, R., Sahasrabudhe, S., Thomas, A., Cannings, R., Gutin, A., Pruss, D., Reid, J., Tavtigian, S., Mitchell, J., El-

dredge, G., Scholl, T., Miller, R. M., Bhatnagar, S., Adey, N., Rubano, T., Tusneem, N., Robinson, R., Feldhaus, J., Macalma, T., Oliphant, A., and Briggs, S. (2002) A draft sequence of the rice genome (*Oryza sativa* L. ssp. *japonica*). *Science* **296,** 92–100
4. Xu, Q., Fu, H. H., Gupta, R., and Luan, S. (1998) Molecular characterization of a tyrosine-specific protein phosphatase encoded by a stress-responsive gene in *Arabidopsis*. *Plant Cell* **10,** 849–857
5. Nakagami, H., Sugiyama, N., Mochida, K., Daudi, A., Yoshida, Y., Toyoda, T., Tomita, M., Ishihama, Y., and Shirasu, K. (2010) Large-scale comparative phosphoproteomics identifies conserved phosphorylation sites in plants. *Plant Physiol.* **153,** 1161–1174
6. van Wijk, K. J., Friso, G., Walther, D., and Schulze, W. X. (2014) Meta-analysis of *Arabidopsis thaliana* phospho-proteomics data reveals compartmentalization of phosphorylation motifs. *Plant Cell* **26,** 2367–2389
7. Ghelis, T. (2011) Signal processing by protein tyrosine phosphorylation in plants. *Plant Signal. Behav.* **6,** 942–951
8. Ghelis, T., Bolbach, G., Clodic, G., Habricot, Y., Miginiac, E., Sotta, B., and Jeannette, E. (2008) Protein tyrosine kinases and protein tyrosine phosphatases are involved in abscisic acid-dependent processes in *Arabidopsis* seeds and suspension cells. *Plant Physiol.* **148,** 1668–1680
9. Fu, X., Richards, D. E., Ait-Ali, T., Hynes, L. W., Ougham, H., Peng, J., and Harberd, N. P. (2002) Gibberellin-mediated proteasome-dependent degradation of the barley DELLA protein SLN1 repressor. *Plant Cell* **14,** 3191–3200
10. Sangwan, V., Foulds, I., Singh, J., and Dhindsa, R. S. (2001) Cold-activation of *Brassica napus* BN115 promoter is mediated by structural changes in membranes and cytoskeleton, and requires Ca^{2+} influx. *Plant J.* **27,** 1–12
11. Ritsema, T., Brodmann, D., Diks, S. H., Bos, C. L., Nagaraj, V., Pieterse, C. M., Boller, T., Wiemken, A., and Peppelenbosch, M. P. (2009) Are small GTPases signal hubs in sugar-mediated induction of fructan biosynthesis? *PLos One* **4,** e6605
12. Yemets, A., Sheremet, Y., Vissenberg, K., Van Orden, J., Verbelen, J. P., and Blume, Y. B. (2008) Effects of tyrosine kinase and phosphatase inhibitors on microtubules in *Arabidopsis* root cells. *Cell Biol. Int.* **32,** 630–637
13. Sheremet, Y. A., Yemets, A. I., Azmi, A., Vissenberg, K., Verbelen, J. P., and Blume, Y. B. (2012) Effects of tyrosine kinase and phosphatase inhibitors on mitosis progression in synchronized tobacco BY-2 cells. *Tsitol. Genet.* **46,** 3–11
14. de la Fuente van Bentem S., and Hirt, H. (2009) Protein tyrosine phosphorylation in plants: more abundant than expected? *Trends Plant Sci.* **14,** 71–76
15. Swatek, K. N., Wilson, R. S., Ahsan, N., Tritz, R. L., and Thelen, J. J. (2014) Multisite phosphorylation of 14-3-3 proteins by calcium-dependent protein kinases. *Biochem. J.* **459,** 15–25
16. Oh, M. H., Wu, X., Kim, H. S., Harper, J. F., Zielinski, R. E., Clouse, S. D., and Huber, S. C. (2012) CDPKs are dual-specificity protein kinases and tyrosine autophosphorylation attenuates kinase activity. *FEBS Lett.* **586,** 4070–4075
17. Nemoto, K., Seto, T., Takahashi, H., Nozawa, A., Seki, M., Shinozaki, K., Endo, Y., and Sawasaki, T. (2011) Autophosphorylation profiling of *Arabidopsis* protein kinases using the cell-free system. *Phytochemistry* **72,** 1136–1144
18. Nozawa, A., Matsubara, Y., Tanaka, Y., Takahashi, H., Akagi, T., Seki, M., Shinozaki, K., Endo, Y., and Sawasaki, T. (2009) Construction of a protein library of *Arabidopsis* transcription factors using wheat cell-free protein production system and its application for DNA binding analysis. *Biosci. Biotechnol. Biochem.* **73,** 1661–1664
19. Sawasaki, T., Ogasawara, T., Morishita, R., and Endo, Y. (2002) A cell-free protein synthesis system for high-throughput proteomics. *Proc. Natl. Acad. Sci. U.S.A.* **99,** 14652–14657
20. Sawasaki, T., Kamura, N., Matsunaga, S., Saeki, M., Tsuchimochi, M., Morishita, R., and Endo, Y. (2008) *Arabidopsis* HY5 protein functions as a DNA-binding tag for purification and functional immobilization of proteins on agarose/DNA microplate. *FEBS Lett.* **582,** 221–228
21. Madin, K., Sawasaki, T., Ogasawara, T., and Endo, Y. (2000) A highly efficient and robust cell-free protein synthesis system prepared from wheat embryos: plants apparently contain a suicide system directed at ribosomes. *Proc. Natl. Acad. Sci. U.S.A.* **97,** 559–564
22. Sawasaki, T., Hasegawa, Y., Tsuchimochi, M., Kamura, N., Ogasawara, T., Kuroita, T., and Endo, Y. (2002) A bilayer cell-free protein synthesis system for high-throughput screening of gene products. *FEBS Lett.* **514,** 102–105
23. Takahashi, H., Ozawa, A., Nemoto, K., Nozawa, A., Seki, M., Shinozaki, K., Takeda, H., Endo, Y., and Sawasaki, T. (2012) Genome-wide biochemical analysis of *Arabidopsis* protein phosphatase using a wheat cell-free system. *FEBS Lett.* **586,** 3134–3141
24. Chiu, W., Niwa, Y., Zeng, W., Hirano, T., Kobayashi, H., and Sheen, J. (1996) Engineered GFP as a vital reporter in plants. *Curr. Biol.* **6,** 325–330
25. Satoh, R., Fujita, Y., Nakashima, K., Shinozaki, K., and Yamaguchi-Shinozaki, K. (2004) A novel subgroup of bZIP proteins functions as transcriptional activators in hypoosmolarity-responsive expression of the *ProDH* gene in *Arabidopsis*. *Plant Cell Physiol.* **45,** 309–317
26. Smith, J. A., Francis, S. H., and Corbin, J. D. (1993) Autophosphorylation: a salient feature of protein kinases. *Mol. Cell. Biochem.* **127,** 51–70
27. Wang, Z. X., and Wu, J. W. (2002) Autophosphorylation kinetics of protein kinases. *Biochem. J.* **368,** 947–952
28. Ali, N., Halfter, U., and Chua, N. H. (1994) Cloning and biochemical characterization of a plant protein kinase that phosphorylates serine, threonine, and tyrosine. *J. Biol. Chem.* **269,** 31626–31629
29. Hrabak, E. M., Chan, C. W., Gribskov, M., Harper, J. F., Choi, J. H., Halford, N., Kudla, J., Luan, S., Nimmo, H. G., Sussman, M. R., Thomas, M., Walker-Simmons, K., Zhu, J. K., and Harmon, A. C. (2003) The *Arabidopsis* CDPK-SnRK superfamily of protein kinases. *Plant Physiol.* **132,** 666–680
30. Blume, Y., Yemets, A., Sheremet, Y., Nyporko, A., Sulimenko, V., Sulimenko, T., and Dráber, P. (2010) Exposure of β-tubulin regions defined by antibodies on an *Arabidopsis thaliana* microtubule protofilament model and in the cells. *BMC Plant Biol.* **10,** 29
31. Blume, Y., Yemets, A., Sulimenko, V., Sulimenko, T., Chan, J., Lloyd, C., and Dráber, P. (2008) Tyrosine phosphorylation of plant tubulin. *Planta* **229,** 143–150
32. Li, R. J., Hua, W., and Lu, Y. T. (2006) *Arabidopsis* cytosolic glutamine synthetase AtGLN1;1 is a potential substrate of AtCRK3 involved in leaf senescence. *Biochem. Biophys. Res. Commun.* **342,** 119–126
33. Masaoka, T., Nishi, M., Ryo, A., Endo, Y., and Sawasaki, T. (2008) The wheat germ cell-free based screening of protein substrates of calcium/calmodulin-dependent protein kinase IIδ. *FEBS Lett.* **582,** 1795–1801
34. Kim, T. W., Guan, S., Sun, Y., Deng, Z., Tang, W., Shang, J. X., Sun, Y., Burlingame, A. L., and Wang, Z. Y. (2009) Brassinosteroid signal transduction from cell-surface receptor kinases to nuclear transcription factors. *Nat. Cell Biol.* **11,** 1254–1260
35. Huang, Y., Li, H., Gupta, R., Morris, P. C., Luan, S., and Kieber, J. J. (2000) ATMPK4, an *Arabidopsis* homolog of mitogen-activated protein kinase, is activated in vitro by AtMEK1 through threonine phosphorylation. *Plant Physiol.* **122,** 1301–1310
36. Sugiyama, N., Nakagami, H., Mochida, K., Daudi, A., Tomita, M., Shirasu, K., and Ishihama, Y. (2008) Large-scale phosphorylation mapping reveals the extent of tyrosine phosphorylation in *Arabidopsis*. *Mol. Syst. Biol.* **4,** 193
37. Ubersax, J. A., and Ferrell, J. E., Jr. (2007) Mechanisms of specificity in protein phosphorylation. *Nat. Rev. Mol. Cell Biol.* **8,** 530–541
38. Oh, M. H., Wang, X., Kota, U., Goshe, M. B., Clouse, S. D., and Huber, S. C. (2009) Tyrosine phosphorylation of the BRI1 receptor kinase emerges as a component of brassinosteroid signaling in *Arabidopsis*. *Proc. Natl. Acad. Sci. U.S.A.* **106,** 658–663
39. Lin, W., Li, B., Lu, D., Chen, S., Zhu, N., He, P., and Shan, L. (2014) Tyrosine phosphorylation of protein kinase complex BAK1/BIK1 mediates *Arabidopsis* innate immunity. *Proc. Natl. Acad. Sci. U.S.A.* **111,** 3632–3637
40. Oh, M. H., Wang, X., Clouse, S. D., and Huber, S. C. (2012) Deactivation of the *Arabidopsis* BRASSINOSTEROID INSENSITIVE 1 (BRI1) receptor kinase by autophosphorylation within the glycine-rich loop. *Proc. Natl. Acad. Sci. U.S.A.* **109,** 327–332
41. Wang, X., Kota, U., He, K., Blackburn, K., Li, J., Goshe, M. B., Huber, S. C., and Clouse, S. D. (2008) Sequential transphosphorylation of the BRI1/BAK1 receptor kinase complex impacts early events in brassinosteroid

signaling. *Dev. Cell* **15,** 220–235
42. Wang, X., Li, X., Meisenhelder, J., Hunter, T., Yoshida, S., Asami, T., and Chory, J. (2005) Autoregulation and homodimerization are involved in the activation of the plant steroid receptor BRI1. *Dev. Cell* **8,** 855–865
43. Hegeman, A. D., Rodriguez, M., Han, B. W., Uno, Y., Phillips, G. N., Jr., Hrabak, E. M., Cushman, J. C., Harper, J. F., Harmon, A. C., and Sussman, M. R. (2006) A phyloproteomic characterization of *in vitro* autophosphorylation in calcium-dependent protein kinases. *Proteomics* **6,** 3649–3664
44. Du, W., Wang, Y., Liang, S., and Lu, Y. T. (2005) Biochemical and expression analysis of an *Arabidopsis* calcium-dependent protein kinase-related kinase. *Plant Sci.* **168,** 1181–1192
45. Hotta, H., Aoki, N., Matsuda, T., and Adachi, T. (1998) Molecular analysis of a novel protein kinase in maturing rice seed. *Gene* **213,** 47–54
46. Lu, Y. T., and Feldman, L. J. (1997) Light-regulated root gravitropism: a role for, and characterization of, a calcium/calmodulin-dependent protein kinase homolog. *Planta* **203,** S91–S97
47. Ma, L., Liang, S., Jones, R. L., and Lu, Y. T. (2004) Characterization of a novel calcium/calmodulin-dependent protein kinase from tobacco. *Plant Physiol.* **135,** 1280–1293
48. Wang, L., Liang, S., and Lu, Y. T. (2001) Characterization, physical location and expression of the genes encoding calcium/calmodulin-dependent protein kinases in maize (*Zea mays* L.). *Planta* **213,** 556–564
49. Zhang, L., Liu, B. F., Liang, S., Jones, R. L., and Lu, Y. T. (2002) Molecular and biochemical characterization of a calcium/calmodulin-binding protein kinase from rice. *Biochem. J.* **368,** 145–157
50. Boudsocq, M., and Sheen, J. (2013) CDPKs in immune and stress signaling. *Trends Plant Sci.* **18,** 30–40
51. Kulik, A., Wawer, I., Krzywińska, E., Bucholc, M., and Dobrowolska, G. (2011) SnRK2 protein kinases: key regulators of plant response to abiotic stresses. *OMICS* **15,** 859–872
52. Engelsberger, W. R., and Schulze, W. X. (2012) Nitrate and ammonium lead to distinct global dynamic phosphorylation patterns when resupplied to nitrogen-starved *Arabidopsis* seedlings. *Plant J.* **69,** 978–995
53. Matten, W. T., Aubry, M., West, J., and Maness, P. F. (1990) Tubulin is phosphorylated at tyrosine by pp60c-src in nerve growth cone membranes. *J. Cell Biol.* **111,** 1959–1970
54. Maness, P. F., and Matten, W. T. (1990) Tyrosine phosphorylation of membrane-associated tubulin in nerve growth cones enriched in pp60c-src. *Ciba Found. Symp.* **150,** 57–69
55. Kilian, J., Whitehead, D., Horak, J., Wanke, D., Weinl, S., Batistic, O., D'Angelo, C., Bornberg-Bauer, E., Kudla, J., and Harter, K. (2007) The AtGenExpress global stress expression data set: protocols, evaluation and model data analysis of UV-B light, drought and cold stress responses. *Plant J.* **50,** 347–363
56. Liu, J., Wang, B., Zhang, Y., Wang, Y., Kong, J., Zhu, L., Yang, X., and Zha, G. (2014) Microtubule dynamics is required for root elongation growth under osmotic stress in Arabidopsis. *Plant Growth Regul.* **74,** 187–192
57. Kudoh, A., Takahama, S., Sawasaki, T., Ode, H., Yokoyama, M., Okayama, A., Ishikawa, A., Miyakawa, K., Matsunaga, S., Kimura, H., Sugiura, W., Sato, H., Hirano, H., Ohno, S., Yamamoto, N., and Ryo, A. (2014) The phosphorylation of HIV-1 Gag by atypical protein kinase C facilitates viral infectivity by promoting Vpr incorporation into virions. *Retrovirology* **11,** 9
58. Masaki, T., Matsunaga, S., Takahashi, H., Nakashima, K., Kimura, Y., Ito, M., Matsuda, M., Murayama, A., Kato, T., Hirano, H., Endo, Y., Lemon, S. M., Wakita, T., Sawasaki, T., and Suzuki, T. (2014) Involvement of hepatitis C virus NS5A hyperphosphorylation mediated by casein kinase I-α in infectious virus production. *J. Virol.* **88,** 7541–7555
59. Rigó, G., Ayaydin, F., Tietz, O., Zsigmond, L., Kovács, H., Páy, A., Salchert, K., Darula, Z., Medzihradszky, K. F., Szabados, L., Palme, K., Koncz, C., and Cséplo, A. (2013) Inactivation of plasma membrane-localized CDPK-RELATED KINASE5 decelerates PIN2 exocytosis and root gravitropic response in Arabidopsis. *Plant Cell* **25,** 1592–1608
60. Wang, Y., Zhang, M., Ke, K., and Lu, Y. T. (2005) Cellular localization and biochemical characterization of a novel calcium-dependent protein kinase from tobacco. *Cell Res.* **15,** 604–612
61. Leclercq, J., Ranty, B., Sanchez-Ballesta, M. T., Li, Z., Jones, B., Jauneau, A., Pech, J. C., Latché, A., Ranjeva, R., and Bouzayen, M. (2005) Molecular and biochemical characterization of LeCRK1, a ripening-associated tomato CDPK-related kinase. *J. Exp. Bot.* **56,** 25–35
62. Lee, S. J., Park, J. H., Lee, M. H., Yu, J. H., and Kim, S. Y. (2010) Isolation and functional characterization of CE1 binding proteins. *BMC Plant Biol.* **10,** 277
63. Liu, H. T., Gao, F., Li, G. L., Han, J. L., Liu, D. L., Sun, D. Y., and Zhou, R. G. (2008) The calmodulin-binding protein kinase 3 is part of heat-shock signal transduction in *Arabidopsis thaliana*. *Plant J.* **55,** 760–773
64. Hua, W., Zhang, L., Liang, S., Jones, R. L., and Lu, Y. T. (2004) A tobacco calcium/calmodulin-binding protein kinase functions as a negative regulator of flowering. *J. Biol. Chem.* **279,** 31483–31494
65. Pandey, S., Tiwari, S. B., Tyagi, W., Reddy, M. K., Upadhyaya, K. C., and Sopory, S. K. (2002) A Ca^{2+}/CaM-dependent kinase from pea is stress regulated and *in vitro* phosphorylates a protein that binds to AtCaM5 promoter. *Eur. J. Biochem.* **269,** 3193–3204
66. Hua, W., Li, R. J., Wang, L., and Lu, Y. T. (2004) A tobacco calmodulin-binding protein kinase (NtCBK2) induced by high-salt/GA treatment and its expression during floral development and embryogenesis. *Plant Sci.* **166,** 1253–1259
67. Das, R., and Pandey, G. K. (2010) Expressional analysis and role of calcium regulated kinases in abiotic stress signaling. *Curr. Genomics* **11,** 2–13
68. Vizcaíno, J. A., Côté, R. G., Csordas, A., Dianes, J. A., Fabregat, A., Foster, J. M., Griss, J., Alpi, E., Birim, M., Contell, J., O'Kelly, G., Schoenegger, A., Ovelleiro, D., Pérez-Riverol, Y., Reisinger, F., Ríos, D., Wang, R., and Hermjakob, H. (2013) The PRoteomics IDEntifications (PRIDE) database and associated tools: status in 2013. *Nucleic Acids Res.* **41,** D1063–D1069